frontiers | Frontiers in Physics

TYPE Brief Research Report
PUBLISHED 01 February 2023
DOI 10.3389/fphy.2023.1124924

OPEN ACCESS

EDITED BY
Sinu Mathew,
Mahatma Gandhi University, India

REVIEWED BY
Jun Kue Park,
Korea Atomic Energy Research Institute (KAERI), South Korea
P. K. Johnny Wong,
Northwestern Polytechnical University, China

*CORRESPONDENCE
Pablo D. Esquinazi,
esquin@physik.uni-leipzig.de

†PRESENT ADDRESS
Markus Stiller, zollsoft GmbH, Jena, Germany

SPECIALTY SECTION
This article was submitted to Condensed Matter Physics, a section of the journal Frontiers in Physics

RECEIVED 15 December 2022
ACCEPTED 16 January 2023
PUBLISHED 01 February 2023

CITATION
Stiller M and Esquinazi PD (2023), Defect-induced magnetism in TiO_2: An example of quasi 2D magnetic order with perpendicular anisotropy.
Front. Phys. 11:1124924.
doi: 10.3389/fphy.2023.1124924

Defect-induced magnetism in TiO_2: An example of quasi 2D magnetic order with perpendicular anisotropy

Markus Stiller† and Pablo D. Esquinazi*

Division of Quantum Magnetism and Superconductivity, Felix-Bloch Institute, University of Leipzig, Leipzig, Germany

Magnetic order at room temperature induced by atomic lattice defects, like vacancies, interstitials, or their pairs, has been observed in a large number of different non-magnetic hosts, such as pure graphite, oxides, and silicon-based materials. High Curie temperatures and time-independent magnetic response at room temperature indicate the extraordinary robustness of this new phenomenon in solid-state magnetism. In this work, we review experimental and theoretical results of pure TiO_2 (anatase), whose magnetic order can be triggered by low-energy ion irradiation. In particular, we discuss the systematic observation of an ultrathin magnetic layer with perpendicular magnetic anisotropy at the surface of this oxide.

KEYWORDS

oxide, 2D magnetic order, defect-induced magnetism, ion irradiation, vacancy–interstitial pairs, surface ferromagnetism

1 Introduction to defect-induced magnetism

Till not so far away in time, solid-state physicists and materials scientists were convinced that to get magnetic order in a solid, one needs a certain amount of magnetic ions, like Fe and Ni, in the atomic lattice. Their amount and environment have a direct influence on the magnetic ordering temperature, i.e., the Curie temperature. This concept has been successfully applied in basic and applied research to get magnetic order in solids, since Heisenberg introduced the idea of exchange interaction between the electron orbits of neighbor magnetic ions [1]. Actually, the changes in the electron orbits produced by a defect, such as a vacancy in its environment, can be substantially large. Therefore, these changes can lead to a non-negligible probability to have a significant local magnetic moment [2–9]. To get magnetic order in a solid through atomic lattice defects or through doping of non-magnetic ions, we need to reach a minimum defect density of the order of (or larger than) ~ 5 at%. The reason is that at this or higher density, the exchange coupling mechanism between the localized magnetic moments at the defects gets robust enough to trigger the alignment between them. Defect engineering is also of significance in two-dimensional samples, as in transition-metal dichalcogenide materials, see, for e.g., the review in [10]. Moreover, magnetic order through Se-vacancies has been recently demonstrated in the VSe_2 monolayer [11]. Ion irradiation can be used in this case to systematically produce a certain kind of vacancy by appropriately choosing the ion and its energy.

2 Emerging ferromagnetic phase through ion irradiation

Ion irradiation is a sophisticated method to systematically produce atomic lattice defects at certain positions and a given density. The main difference between the irradiation of a solid with

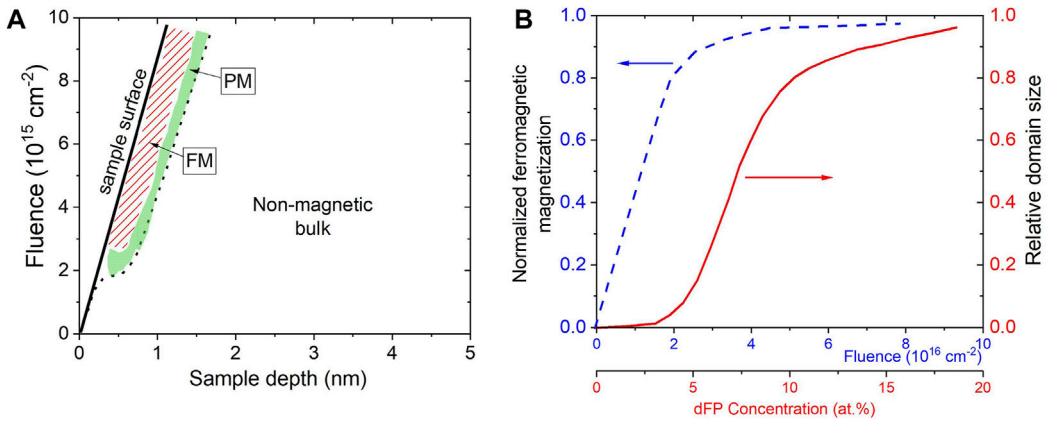

FIGURE 1
(A) Semiquantitative magnetic phase diagram (fluence vs sample depth) for a TiO_2 anatase sample irradiated with Ar^+ ions of 200 eV energy following the results of [25]. The straight line denotes the position of the sample surface, which shifts due to the sputtering. The red region is the ferromagnetic (FM) region, and the green is a paramagnetic (PM) region. The dotted line represents roughly the transition region between a PM and a non-magnetic region, where the mean number of defects created by the irradiation is negligible. The dotted line can be considered the penetration depth of the irradiated ions. **(B)** Blue dashed line represents normalized ferromagnetic magnetization vs Ar^+ fluence or the estimated dFP density in the TiO_2 anatase phase. Red line represents relative FM domain size vs fluence or dFP concentration. The curves represent semiquantitatively the main theoretical results from [25] for the case of irradiation of Ar^+ ions with 200 eV energy in the TiO_2 anatase phase.

different kinds of ions (including protons and electrons) is given by their penetration depth, density, and type of atomic lattice defects produced upon selected energies. Several studies on the subject were published in the past, see, for e.g., [12–18] with Curie temperatures up to 880 K [16, 19].

The possibility to trigger local magnetic moments up to magnetic order by particle irradiation on a given solid, despite its structure, is significant. Starting from proton irradiation of graphite [20–23] and ZnO [4] to Ar^+ irradiation of TiO_2 [24, 25], the number of published works on using irradiation to trigger magnetic order increases steadily.

In this section, we would like to discuss general results following the theoretical works described in Refs [25, 26]. In particular, we discuss here the emergence of the two-dimensional magnetic order at the surface of TiO_2 in its anatase structure, obtained assuming Ar^+ irradiation at low energies $\lesssim$ 200 eV. In general, after ion irradiation with the corresponding fluence and energy to trigger magnetic order, the defect density remains below the threshold where amorphicity grows all over the sample. The magnetic order is in general observed directly after ion irradiation without any further (thermal) treatment.

Which are the main magnetic defects one produces in TiO_2 by Ar^+ irradiation? From the molecular dynamic simulations of collision cascades in TiO_2 anatase given in [25–27], the primary magnetic defects are found to be the so-called di-Frenkel pairs (dFPs), consisting of two Ti atoms displaced into interstitial sites leaving behind two vacancies. Also, oxygen vacancies O_v are created. With the help of density functional theory (DFT) calculations, the magnetic moment of a dFP has been calculated to be 2 μ_B [26] and 1 μ_B [28] for the O_v. The defect formation probabilities for these defects, calculated in [27], are large (~ 40% and ~ 50%, respectively). A diagram of these probabilities for other defects in TiO_2 anatase is shown in Figure 8 in [25]. With the knowledge of these probabilities and using the program SRIM [29], a magnetic phase diagram can be proposed.

Figure 1A shows the expected magnetic phases as a function of the used fluence and sample depth. The magnetic phase diagram resumes the results obtained in [25] for TiO_2 anatase using Ar^+ ions. The absolute values included in the magnetic phase diagram of Figure 1 roughly correspond to the case we discuss here (Ar^+ ions at an energy of ~ 200 eV). The straight line in Figure 1A represents the evolution of the surface position of the TiO_2 sample (which represents a decrease in the total sample thickness) when the ion fluence increases. The main reason for this behavior is surface sputtering, which is non-negligible at low ion energies. Roughly speaking, using SRIM [29], the estimated sputtering is ~ 1 nm/(10^{16} ion/cm^2) [25]. Due to the sputtering, the amorphous surface layer produced by the irradiation is continuously removed. Following [25], from a fluence value of $\sim 4 \times 10^{15}$ cm^{-2}, the defect creation and sputtering processes reach equilibrium, where the volume (and defect density) of the emerging FM phase (red region in Figure 1A) remains constant over the whole fluence range above this value. In this regime, the thickness of the FM phase reaches a value of $d_{FM} \simeq 0.46$ nm, which is about 1/2 of the anatase lattice constant $c = 0.951$ nm along the (001) crystal direction. It means that with an irradiation energy of ~ 200 eV, we expect to have an emerging FM phase at the first ~ two layers of the TiO_2 lattice at its surface.

Deeper in the sample, beyond the ~ 0.5 nm thick FM layer, the density of magnetic defects decreases below the required minimum (~ 5%) to get FM. Instead, a paramagnetic (PM) phase appears (green region in Figure 1A). The dotted line in the diagram represents the transition region between PM and the non-magnetic bulk, which can be interpreted as the mean penetration depth of the Ar^+ ions at 200 eV.

Increasing the defect density leads to a transition from isolated local magnetic moments to a long-ranged ordered phase. How many dFP defects are created in the TiO_2 anatase atomic lattice within the FM phase? This depends on the length scale of the exchange coupling, which determines whether two localized magnetic moments (the dFP in the case of TiO_2) are close enough to each other to ferromagnetically interact. Ref. [25] answered this question within the framework of the

percolation theory, and the main results are shown in Figure 1B. It semiquantitatively shows the theoretical results [25] on the evolution of the FM magnetization and the relative domain size as a function of dFP concentration or fluence for the irradiation of Ar^+ ions at 200 eV. Single pairs of defects interacting ferromagnetically build the smallest ferromagnetic domain. The size of the domains increases with the increase in the defect density as shown by the red line in Figure 1B. For a density of dFP $\gtrsim$ 10 at%, the domain size tends to saturate at the sample size (relative domain size 1). At this defect concentration, the FM magnetization (blue dashed line in Figure 1B) tends to reach its saturation.

The magnetic percolation transition as a function of the fluence of Ar^+ ions (or defect density) was experimentally verified by measuring the remanent magnetic moment at the zero field of TiO_2 thin films as a function of the fluence. It follows the expected critical behavior for a percolation transition of a magnetic bilayer system (see Figure 13 in [25]). In the next section, we review the experimental evidence for the appearance of this 2D magnetic system with the interesting property of having the magnetization easy axis normal to the main sample surface.

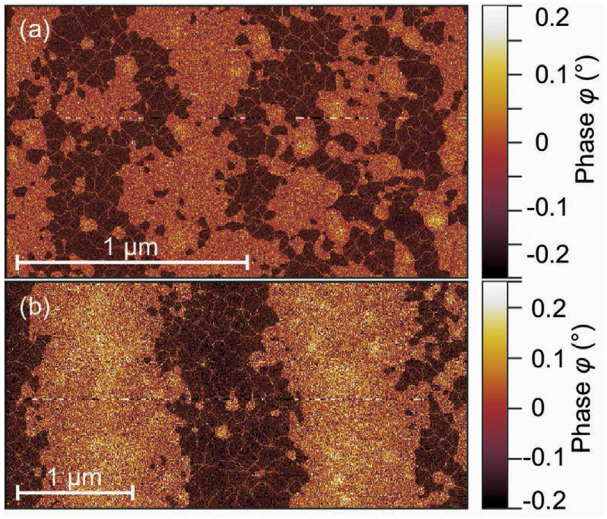

FIGURE 2
Magnetic force microscopy measurements at two different positions **(A)** and **(B)** of a fully irradiated and otherwise untreated anatase thin film. The TiO_2 thin film was irradiated with Ar^+ ions with a fluence of ~ 10^{16} cm^{-2} and energy of 200 eV. The magnetic domains have been segmented with a barrier of 40% and a Gaussian smoothing factor of 8 px.

3 Evidence for a two-dimensional ferromagnetic phase with the out-of-plane easy axis

3.1 Reasons for the magnetic anisotropy

As indicated previously, following theoretical and experimental results, at a low ion energy of 200 eV, the magnetically ordered phase appears at the first two layers of the TiO_2 anatase surface. If we irradiate TiO_2 with Ar^+ ions of higher energy (e.g., 500 eV), the magnetic anisotropy changes and the magnetization easy-axis points become parallel to the sample surface [25, 26]. This evidence clearly indicates that the negative magnetic anisotropy energy (MAE) found at low irradiation energies is directly related to the two-dimensionality of the ferromagnetic phase produced at the surface of the TiO_2 sample. The localized magnetic moments of the dFP defect at the (001) anatase surface of the measured samples exist at the two interstitial Ti places. One of the interstitials $Ti_{i,2}$ is located at the first surface layer whereas the other interstitial $Ti_{i,1}$ on the second layer. According to DFT electronic structure calculations using the full-potential linearized augmented plane wave (FLAPW) method, the magnetic defect $Ti_{i,1}$ shows a spin structure similar to that in the bulk, whereas the $Ti_{i,2}$ defect shows a completely different spin polarization with a negative MAE due to the reduced coordination of the surface [25]. Increasing the magnetically ordered volume inside the sample by increasing the irradiation energy results in smaller relative contribution of this magnetic surface to the total magnetization, and the magnetic anisotropy turns to positive.

The first clear hints for the unusual magnetic anisotropy of the TiO_2 thin films after irradiation were obtained by SQUID angle-dependent magnetization measurements [24]. This interesting finding was supported a few years later through similar SQUID measurements of new TiO_2 thin films irradiated at different energies [25, 26]. We would like to emphasize that the main results were obtained from magnetic hysteresis loops, obtained applying external magnetic fields parallel and perpendicular to the film surface of irradiated TiO_2 samples using a SQUID magnetometer. The total magnetic anisotropy energy was obtained from the difference between the areas of the two first field (virgin)-dependent curves, for more details, see Ref [25] and its supplementary information [30]. The magnetization results show that the MAE for the 200 eV Ar^+-irradiated sample is negative with a value of MAE ~ − 0.03 mJ/cm^2 nearly independent of the irradiated fluence up to ~ 3×10^{16} cm^{-2} [25], which is in agreement with the predicted behavior given by the red area in Figure 1A. In the next section, we discuss the visualization of magnetic domains *via* MFM, supporting the anomalous MAE of irradiated TiO_2. It is worth to note that perpendicular magnetic anisotropy has been reported in Cr_3Te_4 monolayers, which was triggered in this case not by atomic lattice defects in the material itself but by an interfacial effect between the monolayer and graphite [31].

3.2 Magnetic force microscopy

Thin films of anatase, prepared by pulsed laser deposition on the $LaAlO_3$ substrate, have been irradiated with low-energy ions and measured using magnetic force microscopy (MFM) [26]. Previously conducted SQUID measurements showed a low remanence; thus, we expect randomly distributed magnetic domains at the anatase surface. Figures 2A,B show MFM measurements at two different positions, and the magnetic domains as well as their out-of-plane character can clearly be recognized. An in-plane domain structure would only be visible at the domain walls as the out-of-plane field vanishes within the domains.

In order to examine the possibility for controlled magnetic manipulation at the surface of the anatase thin film, the samples were patterned using electron beam lithography. Therefore, a film was

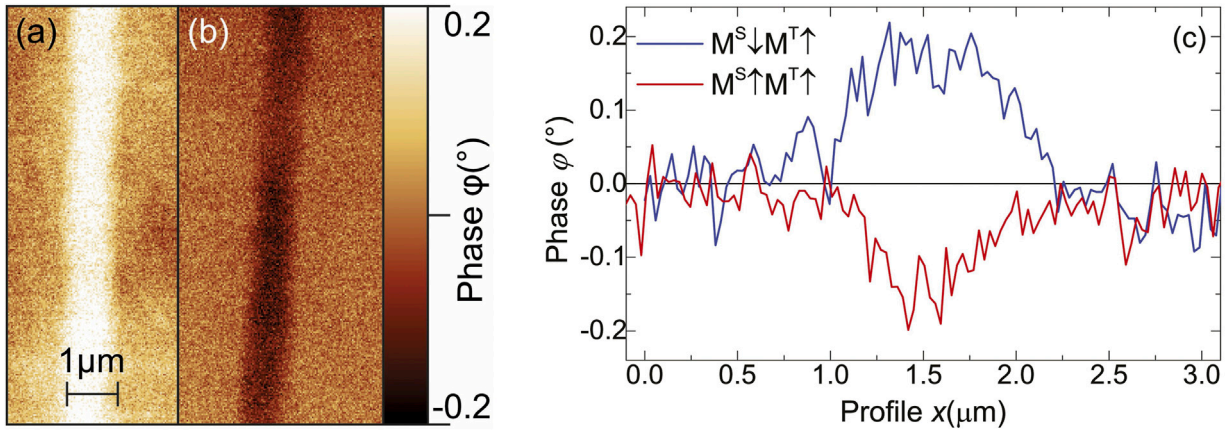

FIGURE 3
Magnetic force microscopy measurements of the sample (M^S) and tip (M^T) magnetization in antiparallel **(A)** and parallel **(B)** directions with respect to each other; **(C)** corresponding line scans.

covered with a resist layer, and electron beam lithography was used to prepare a mask. The resulting irradiated lines or stripes have a width of ≈ 750 nm. After irradiation with low-energy argon ions, the whole mask was completely removed, and the sample was magnetized using a permanent magnet with a magnetic field aligned perpendicular to the sample surface and two magnetization directions: parallel and antiparallel to the tip magnetization. No external field was applied during the measurement [26]. The results are shown in Figures 3A,B and present a clear MFM signal corresponding to the two out-of-plane magnetic field directions; the area of the thin film, which was not irradiated, does not show any MFM response. The corresponding phase line scans normal to the main length of the FM stripes in Figures 3A,B are shown in Figure 3C.

4 Conclusion

In conclusion, it has been shown that ferromagnetism at room temperature with perpendicular magnetic anisotropy can be induced in anatase after irradiating the sample with low-energy ions. The used method is remarkably simple and cheap compared to other experimental methods to produce perpendicular magnetic anisotropy, such as magnetic heterostructures[32]. The irradiation strategy is similar to the doping approach used in the semiconductor industry. However, the advantage of our method relays in its efficiency and the possibility to easily combine with other techniques, as electron beam lithography, allowing the production of arbitrary magnetic patterns with 2D perpendicular magnetic anisotropy.

Data availability statement

The raw data supporting the conclusion of this article will be made available by the authors, without undue reservation.

Author contributions

MS: measurements, sample preparation, writing and correcting the manuscript, and methodology. PDE: writing the manuscript, conceptualization, and funding acquisition. All authors have read and agreed to the published version of the manuscript.

Funding

Part of this study was supported by the DFG, under Project No. 31047526, and SFB 762: "Functionality of oxide interfaces," project B1.

Acknowledgments

The authors acknowledge the support from the German Research Foundation (DFG) and Universität Leipzig for the program of Open Access Publishing.

Conflict of interest

The authors declare that the research was conducted in the absence of any commercial or financial relationships that could be construed as a potential conflict of interest.

Publisher's note

References

1. Heisenberg W. Zur Theorie des Ferromagnetismus. *Z Phys* (1928) 49:619–36.

2. Khalid M, Ziese M, Setzer A, Esquinazi P, Lorenz M, Hochmuth H, et al. Defect-induced magnetic order in pure ZnO films. *Phys Rev B* (2009) 80:035331. doi:10.1103/PhysRevB.80.035331

3. Fischer G, Sanchez N, Adeagbo W, Lüders M, Szotek Z, Temmerman WM, et al. Room-temperaturep-induced surface ferromagnetism: First-principles study. *Phys Rev B* (2011) 84:205306. doi:10.1103/physrevb.84.205306

4. Lorite I, Straube B, Ohldag H, Kumar P, Villafuerte M, Esquinazi P, et al. Advances in methods to obtain and characterise room temperature magnetic ZnO. *Appl Phys Lett* (2015) 106:082406. doi:10.1063/1.4913763

5. Esquinazi PD, Hergert W, Stiller M, Botsch L, Ohldag H, Spemann D, et al. Defect-induced magnetism in nonmagnetic oxides: Basic principles, experimental evidence, and possible devices with ZnO and TiO_2. *Phys Status Solidi B* (2020) 257:1900623. doi:10.1002/pssb.201900623

6. Volnianska O, Boguslawski P. Magnetism of solids resulting from spin polarization of *p* orbitals. *J Phys Condens Matter* (2010) 22:073202. doi:10.1088/0953-8984/22/7/073202

7. Ogale SB. Dilute doping, defects, and ferromagnetism in metal oxide systems. *Adv Mater* (2010) 22:3125–55. doi:10.1002/adma.200903891

8. Stoneham M. The strange magnetism of oxides and carbons. *J Phys Condens Matter* (2010) 22:074211. doi:10.1088/0953-8984/22/7/074211

9. Esquinazi P, Hergert W, Spemann D, Setzer A, Ernst A. Defect-induced magnetism in solids. *Magnetics, IEEE Trans*(2013) 49:4668–74. doi:10.1109/TMAG.2013.2255867

10. Liang Q, Zhang Q, Zhao X, Liu M, Wee ATS. Defect engineering of two-dimensional transition-metal dichalcogenides: Applications, challenges, and opportunities. *ACS Nano* (2021) 15:2165–81. doi:10.1021/acsnano.0c09666

11. Chua R, Yang J, He X, Yu X, Yu W, Bussolotti F, et al. Can reconstructed Se-deficient line defects in monolayer VSe2 induce magnetism? *Adv Mater* (2020) 32:2000693. doi:10.1002/adma.202000693

12. Hong NH, Sakai J, Poirot N, Brizé V. Room-temperature ferromagnetism observed in undoped semiconducting and insulating oxide thin films. *Phys Rev B* (2006) 73:132404–4. doi:10.1103/PhysRevB.73.132404

13. Zhou S, Čižmár E, Potzger K, Krause M, Talut G, Helm M, et al. Origin of magnetic moments in defective TiO_2 single crystals. *Phys Rev B* (2009) 79:113201–4. doi:10.1103/PhysRevB.79.113201

14. Cruz MM, Silva RC, Franco N, Godinho M. Ferromagnetism induced in rutile single crystals by argon and nitrogen implantation. *J Phys Condensed Matter* (2009) 21:206002–8. doi:10.1088/0953-8984/21/20/206002

15. Thakur H, Thakur P, Kumar R, Brookes NB, Sharma KK, Singh AP, et al. Irradiation induced ferromagnetism at room temperature in TiO_2 thin films: X-Ray magnetic circular dichroism characterizations. *Appl Phys Lett* (2011) 98:192512–3. doi:10.1063/1.3592250

16. Yoon SD, Chen Y, Yang A, Goodrich TL, Zuo X, Ziemer K, et al. Magnetic semiconducting anatase $TiO_{2-\delta}$ grown on (100) $LaAlO_3$ having magnetic order up to 880k. *J Magnetism Magn Mater* (2007) 309:171–5. doi:10.1016/j.jmmm.2006.05.014

17. Li DX, Qin XB, Zheng LR, Li YX, Cao XZ, Li ZX, et al. Defect types and room-temperature ferromagnetism in undoped rutile TiO_2 single crystals. *Chin Phys B* (2013) 22:037504–4. doi:10.1088/1674-1056/22/3/037504

18. Vázquez-Robaina O, Cabrera AF, Cruz AF, Torres CER. Observation of room-temperature ferromagnetism induced by high-pressure hydrogenation of anatase TiO_2. *J Phys Chem C* (2021) 125:14366–77. doi:10.1021/acs.jpcc.1c00124

19. Yoon SD, Chen Y, Yang A, Goodrich TL, Zuo X, Arena DA, et al. Oxygen-defect-induced magnetism to 880 K in semiconducting anatase $TiO_{2-\delta}$ films. *J Phys Condensed Matter* (2006) 18:L355–61. doi:10.1088/0953-8984/18/27/L01

20. Esquinazi P, Spemann D, Höhne R, Setzer A, Han KH, Butz T. Induced magnetic ordering by proton irradiation in graphite. *Phys Rev Lett* (2003) 91:227201. doi:10.1103/PhysRevLett.91.227201

21. Ohldag H, Tyliszczak T, Höhne R, Spemann D, Esquinazi P, Ungureanu M, et al. π-Electron ferromagnetism in metal-free carbon probed by soft X-ray dichroism. *Phys Rev Lett* (2007) 98:187204. doi:10.1103/PhysRevLett.98.187204

22. Ohldag H, Esquinazi P, Arenholz E, Spemann D, Rothermel M, Setzer A, et al. The role of hydrogen in room-temperature ferromagnetism at graphite surfaces. *New J Phys* (2010) 12:123012. doi:10.1088/1367-2630/12/12/123012

23. Spemann D, Esquinazi P. Basic Physics of Functionalized Graphite, In: *Evidence for magnetic order in graphite from magnetization and transport measurementsSpringer International Publishing AG Switzerland)*. P Esquinazi, editor. *Springer series in materials science*, 244 (2016). p. 45–76. doi:10.1007/978-3-319-39355-1_3

24. Stiller M, Barzola-Quiquia J, Esquinazi P, Spemann D, Meijer J, Lorenz M, et al. Strong out-of-plane magnetic anisotropy in ion irradiated anatase TiO_2 thin films. *AIP Adv* (2016) 6:125009. doi:10.1063/1.4971794

25. Botsch L, Esquinazi PD, Bundesmann C, Spemann D. Toward a systematic discovery of artificial functional magnetic materials. *Phys Rev B* (2021) 104:014428. doi:10.1103/PhysRevB.104.014428

26. Stiller M, N'Diaye AT, Ohldag H, Barzola-Quiquia J, Esquinazi PD, Amelal T, et al. Titanium 3*d* ferromagnetism with perpendicular anisotropy in defective anatase. *Phys Rev B* (2020) 101:014412. doi:10.1103/PhysRevB.101.014412

27. Robinson M, Marks N, Lumpkin G. Structural dependence of threshold displacement energies in rutile, anatase and brookite TiO_2. *Mater Chem Phys* (2014) 147:311–8. doi:10.1016/j.matchemphys.2014.05.006

28. Li QK, Wang B, Woo CH, Wang H, Zhu ZY, Wang R. Origin of unexpected magnetism in Cu-doped TiO_2. *Europhysics Lett (Epl)* (2007) 81:17004. doi:10.1209/0295-5075/81/17004

29. Ziegler JF, Biersack JP, Ziegler MD. *SRIM - the stopping and range of ions in matter*. SRIM Co. (2008). See also the simulation software IIS available at: http://www.ele.uva.es/jesman/iis.html (which has some advantages in comparison with the usual SRIM simulation).

30. Botsch L, Esquinazi PD, Bundesmann C, Spemann D (2021). See Supplemental Material: for full magnetic hysteresis curves and details on obtaining the magnetic anisotropy energy. Availble at: http://link.aps.org/supplemental/10.1103/PhysRevB.104.014428.

31. Chua R, Zhou J, Yu X, Yu W, Gou J, Zhu R, et al. Room temperature ferromagnetism of monolayer chromium telluride with perpendicular magnetic anisotropy. *Adv Mater* (2021) 33:2103360. doi:10.1002/adma.202103360

32. Li W, Zeng Y, Zhao Z, Zhang B, Xu J, Huang X, et al. 2D magnetic heterostructures and their interface modulated magnetism. *ACS Appl Mater Inter* (2021) 13:50591–601. doi:10.1021/acsami.1c11132